

Characterization of Regulatory Volume Behavior by Fluorescence Quenching in Human Corneal Epithelial Cells

J.E. Capó-Aponte¹, P. Iserovich², P.S. Reinach¹

¹Department of Biological Sciences, College of Optometry, State University of New York, New York, NY 10036, USA

²Department of Ophthalmology, College of Physicians and Surgeons, Columbia University, New York, NY 10032, USA

Received: 10 June 2005/Revised: 1 October 2005

Abstract. An in-depth understanding of the mechanisms underlying regulatory volume behavior in corneal epithelial cells has been in part hampered by the lack of adequate methodology for characterizing this phenomenon. Accordingly, we developed a novel approach to characterize time-dependent changes in relative cell volume induced by anisosmotic challenges in calcein-loaded SV40-immortalized human corneal epithelial (HCE) cells with a fluorescence microplate analyzer. During a hypertonic challenge, cells shrank rapidly, followed by a temperature-dependent regulatory volume increase (RVI), $\tau_c = 19$ min. In contrast, a hypotonic challenge induced a rapid ($\tau_c = 2.5$ min) regulatory volume decrease (RVD). Temperature decline from 37 to 24°C reduced RVI by 59%, but did not affect RVD. Bumetanide (50 μ M), ouabain (1 mM), DIDS (1 mM), EIPA (100 μ M), or Na⁺-free solution reduced the RVI by 60, 61, 39, 32, and 69%, respectively. K⁺, Cl⁻ channel and K⁺-Cl⁻ cotransporter (KCC) inhibition obtained with either 4-AP (1 mM), DIDS (1 mM), DIOA (100 μ M), high K⁺ (20 mM) or Cl⁻-free solution, suppressed RVD by 42, 47, 34, 52 and 58%, respectively. KCC activity also affects steady-state cell volume, since its inhibition or stimulation induced relative volume alterations under isotonic conditions. Taken together, K⁺ and Cl⁻ channels in parallel with KCC activity are important mediators of RVD, whereas RVI is temperature-dependent and is essentially mediated by the Na⁺-K⁺-2Cl⁻ cotransporter (Na⁺-K⁺-2Cl⁻) and the Na⁺-K⁺ pump. Inhibition of K⁺ and Cl⁻ channels and KCC but not Na⁺-K⁺-2Cl⁻ affect steady-state cell volume under isotonic conditions. This is the first report that KCC activity is required for HCE cell volume regulation and maintenance of steady-state cell volume.

Key words: Human corneal epithelial cells — Anisosmotic challenge — Cell volume regulation — Calcein fluorescence quenching — Microplate analyzer — K⁺-Cl⁻ cotransporter

Introduction

The corneal epithelial barrier properties protect the tissue from damage resulting from exposure to noxious agents, toxins and environmental insults. This function depends on tissue integrity. Such protection preserves corneal refractive power and transparency, which can be challenged by exposure to an anisosmotic stress.

The ability of the corneal epithelium to provide these functions may be repeatedly challenged by variations in tear film osmolarity. For example, swimming in either sea water or fresh water exposes the corneal epithelium to an anisosmotic challenge. In addition, throughout the day, significant variations in tear film osmolarity often occur. In individuals suffering from certain dry eye conditions, the corneal epithelium may be exposed to even larger localized increases in tear film osmolarity and discontinuities in coverage of the underlying epithelial layer (Farris, 1994). Therefore, to prevent disruption of corneal epithelial layer integrity, adequate activation of regulatory volume mechanisms is essential. Otherwise, a dysfunctional regulatory volume response could possibly lead to epithelial erosion and corneal opacity.

Cellular regulatory volume response entails the restoration of isotonic volume by either active uptake or extrusion of osmolytes. The process that elicits osmolyte uptake is referred to as a regulatory volume increase (RVI), whereas the response resulting in osmolyte loss is designated as regulatory volume decrease (RVD) (Kregenow, 1971; Grinstein, Dupre &

Rothstein, 1982). There is clear qualitative evidence that the corneal epithelium undergoes RVD and RVI responses based on measurements of changes in light scattering (Wu et al., 1997; Bildin et al., 1998). However, quantification of the kinetic parameters is required to fully analyze the ion transport processes underlying these responses.

For cells to return to isotonic volume during anisotonic stress, the activity of specific ion channels and transporters needs to be altered. For example, in many cell types, including human corneal epithelial (HCE) cells, RVI is associated with the stimulation of the $\text{Na}^+\text{-K}^+$ pump and $\text{Na}^+\text{-K}^+\text{-2Cl}^-$ cotransporter (NKCC) activity (Linderholm, 1954; Geck et al., 1980; Bonanno, Klyce & Cragoe, 1989; Russell, 2000; Bildin et al., 2003; Candia, 2004; Fischbarg & Maurice, 2004; Strange, 2004). $\text{Na}^+\text{/H}^+$ (NHE) and $\text{Cl}^-/\text{HCO}_3^-$ exchangers are also present in corneal epithelial cells and perhaps contribute to RVI. NHE produces a net influx of ions by coupling with the $\text{Cl}^-/\text{HCO}_3^-$ anion exchanger (Bonanno, 1991; Williams & Watsky, 2004). Five different NHE isoforms have been identified (i.e., 1–5). The NHE-2 exchanger subtype is involved in volume regulation of bovine corneal epithelium (Torres-Zamorano, Ganapathy & Reinach, 1993; Reinach, Ganapathy & Torres-Zamorano, 1994).

In many cell types, RVD can be accounted for by net potassium (K^+) and chloride (Cl^-) efflux (Wang, Chen & Jacob, 2000; Wang et al., 2002). Among the K^+ channels characterized in corneal epithelial cells are the large-conductance K^+ channels (BK) located in the basolateral membrane (Rae, Dewey & Rae, 1992) and voltage-gated K^+ channels (Kv) in the apical membrane (Takahira et al., 2001). Specifically, Kv3.4 is functionally expressed in the cell membrane of rat and rabbit corneal epithelial (RCE) cells (Roderick et al., 2003; Wang, Li & Lu, 2003; Wang, Fyffe & Lu, 2004) and provides an essential contribution to RVD. In addition to the involvement of the Kv channel in cell volume regulation, it has a crucial role in many other cell functions, including cell proliferation (Shen et al., 2000; Wang et al., 2002; Pardo, 2004) and apoptosis (Lu, Wang & Shell, 2003; Wang et al., 2003).

Chloride efflux pathways that have been identified in the corneal epithelial cells include the cAMP-dependent cystic fibrosis transmembrane conductance regulator protein (CFTR)-mediated Cl^- channel and ClC-3 , an outwardly rectifying Cl^- channel (Al-Nakkash et al., 2004; Levin & Verkman, 2005). The gene expression for the Ca^{2+} -activated Cl^- channel, ClCA2 , was shown in HCE cells; however, the involvement of this channel in volume regulation has not been characterized (Itoh et al., 2000). As K^+ and Cl^- efflux underlies RVD, this response may be modulated through receptor-mediated control of these pathways. However, there are no studies describing such type of control.

Another important RVD-mediating mechanism is the electroneutral $\text{K}^+\text{-Cl}^-$ cotransporter (KCC), which has been identified in erythrocytes, vascular smooth muscle, cardiomyocytes, cultured lens epithelial, cervical and ovarian cancer cells (Diecke & Beyer-Mears, 1997; Taouil & Hannaert, 1999; Di Fulvio et al., 2001; Lauf et al., 2001; Lytle & McManus, 2002; Culliford et al., 2003; Shen et al., 2003, 2004; Joiner et al., 2004). Four different KCC isoforms (KCC1–4) have been identified in mammalian cells. KCC1 serves primarily as a cell volume regulator, while KCC3 has been implicated in cell growth regulation and cell cycle progression (Shen et al., 2001; Di Fulvio et al., 2003). Hypotonic-induced KCC activation can be blocked by the widely used inhibitor [(dihydroindenyl)oxy] alkanoic acid (DIOA) (Diecke & Beyer-Mears, 1997; Culliford et al., 2003; Shen et al., 2003, 2004), whereas KCC is stimulated under isotonic conditions by its known activator *N*-ethylmaleimide (NEM) (Diecke & Beyer-Mears, 1997; Di Fulvio et al., 2001, 2003; Culliford et al., 2003). To our knowledge there are no reports describing KCC activity in HCE cells.

A number of different approaches have been used to measure alleged changes in relative volume of adherent cellular layers, including cell morphometry, light scattering, and changes of trapped intracellular cation concentration as an index of volume alterations (Echevarria et al., 1993; McManus et al., 1993; Alvarez-Leefmans, 1995; Verkman, 2000). Recently, a more adequate and less cumbersome methodology based on self-quenching of calcein fluorescence was introduced to monitor relative cell volume changes (Hamann et al., 2002). As there is an inverse relationship between intracellular calcein concentration and relative cell volume, an increase in dye concentration resulting from cell volume reduction produces a near linear decline in fluorescence and vice versa. Fluorescence microscopy of calcein-loaded cells has been used to evaluate time-dependent changes in relative volume. Despite these advantages, fluorescence microscopy has several drawbacks, such as high excitation light intensity and limited amounts of experimental data per measuring session. Dye losses over extended measurement periods combined with bleaching may induce significant variations in the results. Such variations may in turn make it more time-consuming to establish whether a specific condition induces a significant difference in regulatory volume behavior.

We describe here a relatively simple approach to monitor relative cell volume changes in calcein-loaded HCE cells using a fluorescence microplate analyzer. Advantages of this method include the ability to minimize bleaching by using low level of light intensity for dye excitation, higher throughput allowing the assessment in parallel of many samples exposed to a number of different conditions in

parallel, which markedly improves the quality of the results. With this technique, we quantified RVD and RVI responses to an anisotonic challenge in SV40-immortalized HCE cells and identified the involvement of KCC in the RVD process during a hypotonic challenge and the temperature dependence of RVI. Furthermore, roles for K^+ and Cl^- channels and KCC in maintaining steady-state cell volume under isotonic conditions were identified.

Materials and Methods

CELL CULTURE

SV40-immortalized HCE cells were kindly donated by Dr. Araki-Sasaki (Kinki University, Hyogo, Japan). This cell line exhibits phenotypic and functional properties similar to those of its primary culture counterpart, while allowing continuous growth for over 400 generations (Araki-Sasaki et al., 1995; Huhtala et al., 2002). HCE cells were cultured in Dulbecco's modified Eagle's medium (DMEM/F12) supplemented with 10% fetal bovine serum (FBS), 5 ng/ml epidermal growth factor (EGF), 5 μ g/ml insulin and 40 μ g/ml gentamicin. Cells were cultivated in 25 cm^2 plastic culture flasks (Falcon, Lincoln Park, NJ) in a humidified 5% CO_2 and 95% atmospheric air incubator at 37°C. Cells for microplate analyzer experiments were subcultured onto 24-well plates (MULTIWELL™ Tissue Culture Plates Falcon, Lincoln Park, NJ) 15 mm in diameter at an initial density of about 10^4 cells/well in 0.2 ml aliquots of cell suspension supplemented with 0.5 ml DMEM/F12 and grown to 80–90% confluence for 24 h prior to the experiment as done previously employing light scattering in the same cell type (Bildin et al., 1998; Wu et al., 1997). For microscopy experiments, cells were harvested from the flask and plated on 22-mm diameter glass coverslips (Fisher Scientific, Pittsburgh, PA). The cells were allowed to attach, then supplemented with 2 ml DMEM/F12 and cultured until they reached 80–90% confluence for 24 h prior to the experiment.

REAGENTS AND EXPERIMENTAL SOLUTIONS

Calcein-AM was purchased from Molecular Probes (Eugene, OR). Dimethyl sulfoxide (DMSO), bumetanide, ouabain, 4,4'-diisothiocyanostilbene-2,2'-disulfonic acid (DIDS), ethylisopropylamiloride (EIPA), glybenclamide, niflumic acid, $BaCl_2$, 4-aminopyridine (4-AP), tetraethylammonium chloride (TEA), *N*-ethylmaleimide (NEM), and [(dihydroindenyl) oxy] alkanic acid (DIOA) were purchased from Sigma-Aldrich (St. Louis, MO). Control (isotonic, 300 mOsm) solution contained (mM): NaCl 147.8, KCl 4.7, $MgCl_2 \cdot 6H_2O$ 0.4, glucose 5.5, $CaCl_2$ 1.8, and HEPES Na 5.3. High K^+ solution (20 mM) prepared by isosmolar replacement had similar composition to the control solution, except NaCl concentration was decreased to 132.8 mM and KCl concentration was increased to 20 mM. Nominally Na^+ -free solution was composed of (mM): *N*-methyl-D-glucamine 247.1, KCl 2.5, $MgCl_2 \cdot 6H_2O$ 2.0, glucose 5.0, $CaCl_2$ 5.4, and HEPES free acid 5.3. Cl^- -free solutions contained (mM): sodium cyclamate 134.6, K_2SO_4 2.5, $MgSO_4$ 2.0, glucose 5.0, $CaSO_4$ 5.4, HEPES Na 5.3. For microscopy experiments, perfused hypertonic solution (600 mOsm) was prepared by adding 300 mM sucrose to isotonic solution. Hypotonic solution (150 mOsm) has similar composition as the isotonic solution except NaCl was lowered to 66.3 mM. During microplate analyzer experiments, hypertonic and hypotonic conditions were obtained by adding required aliquots of 600 mOsm hypertonic solution or de-ionized distilled water, respectively. Sham experiments were

performed to establish and validate target osmolarity of all solutions and adjusted pH to 7.4. Preliminary experiments showed that the dilution or solution replacement method yielded similar volume responses. Nevertheless, the dilution method permits a more expeditious osmolarity change. Even though bathing solution dilution results in large decreases in ionic composition, the resulting ionic concentrations are still above the reported apparent K_m values for the various ion transporters evaluated in this study. Osmolarity of solutions was verified based on measurements of freezing-point depression (μ Osmette OsmoMeter, Precision System, Natick, MA). All solutions and inhibitors were freshly prepared prior to experimentation.

CELL VOLUME MEASUREMENT BY MICROPLATE ANALYZER

A Fusion™ Universal Microplate Analyzer (Perkin-Elmer, Boston, MA) was used to record fluorescence intensity of HCE cells at 485 nm excitation and 530 nm emission. This automated system allows for maximal performance of the fluorescence assay by reducing background intensity and eliminating crosstalk from adjacent wells in a multiwell plate. In addition, this system has an integrated temperature control module.

For this experimental setting, we used cells grown in 24-well plates as previously described. The growth medium was replaced with isotonic solution containing 10 μ M calcein-AM for 60 min at 37°C. Cells were washed twice and then incubated with 200 μ L isotonic solution (300 mOsm) per well with or without inhibitors prior to an experiment for 30 min. Cells were incubated for 30 min in isotonic solution based on the results of initial experiments. After application of inhibitors of interest under isotonic conditions, at least 20 min was required for cells to reach a new steady-state volume (see Fig. 4A).

Readings were taken every 30 s (200 ms exposure per well followed by a 10 s delay prior to initiating the next 24-well reading cycle), set at illumination intensity level 5 and high sensitivity. Calibration experiments showed these values were best for yielding an optimal signal without inducing appreciable photodynamic damage and dye bleaching. Illumination was directed from the bottom of the chamber, and signal readout was monitored from the same side of the chamber.

Prior to an experiment, initial fluorescence changes under isotonic conditions were recorded and later used to calculate fluorescence drift correction (Alvarez-Leefmans, 1995; Hamann, 2002). The bathing osmolarity of each well was rapidly adjusted to desired osmolarity by addition of prewarmed solution with a multichannel pipettor. The attainment of the desired osmolarity and pH was validated in sham procedures. Fluorescence readings were repeated at 30 s intervals, unless otherwise indicated, and computer processed.

CELL VOLUME MEASUREMENT BY FLUORESCENCE MICROSCOPY

Fluorescence intensity changes induced by anisotonic challenges were monitored as an index of relative cell volume changes with a Nikon Diaphot 200 inverted microscope coupled to an IC-200 charge-coupled device (CCD) camera (#1400, Xillix Microimager, Vancouver, British Columbia). HCE cells were grown on 22-mm diameter glass coverslips and loaded with 10 μ M calcein-AM as described above. Coverslips were mounted in a microperfusion chamber placed on the stage of the inverted microscope. Cells were continuously superfused with isotonic solution (37°C) fed into the chamber by gravity at a rate of 50 μ L/s. The volume of the chamber (500 μ L) was exchanged in approximately 10 s during the anisotonic challenges.

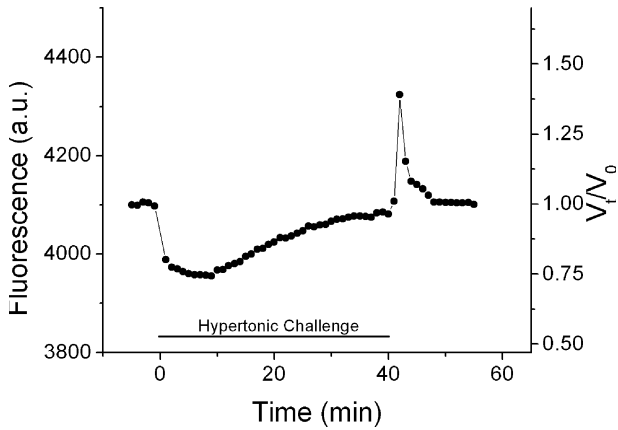


Fig. 1. Relative cell volume changes. This figure shows a representative example of fluorescence (*left axis*) and converted relative cell volume (*right axis*) changes in a calcein-loaded HCE cell obtained with the fluorescence microplate analyzer as determined by Eq. 1. Cells were initially exposed to isotonic solution for 5 min, followed by a 50% hypertonic challenge (indicated by *horizontal line*). After cells have recovered to their initial volume, while exposed to hypertonic solution, they were re-exposed to isotonic volume, which induced cell swelling, followed by post-RVI RVD.

The light source was a 75-W xenon-arc lamp, which was directed through a 490 nm excitation filter (Zeiss). Light pulses lasting 200 ms were delivered every 15 s. A fast shutter that remained closed between excitation pulses was used to reduce photobleaching and photodynamic damage to the cells. The emitted light (520 nm) was detected with a CCD camera. Cells were visualized with a Nikon 40× Fluor oil immersion objective (NA = 1.3) and fluorescence intensity from selected cells was recorded with Ratio Tool™ software (ISee Imaging System, Raleigh, NC).

RELATIVE VOLUME DETERMINATION

The conversion of fluorescence values to relative cell volume requires the determination of the relationship between normalized drift-corrected fluorescence (F_t/F_0) during steady-state volume and the reciprocal of the relative osmotic pressure of the external solution (π_0/π_t). The resultant is a linear relationship, indicating that there is a correspondence between relative changes in fluorescence and changes in cell volume. The conversion of fluorescence to relative cell volume was done by applying equation (1) (Alvarez-Leefmans, 1995; Hamann, 2002).

$$V_t/V_0 = [(F_t/F_0) - f_b]/(1 - f_b) \quad (1)$$

where V_t is the cell water volume at time t , V_0 is V_t at $t = 0$. F_0 is the fluorescence of cells in isotonic solution having osmotic pressure π_0 and F_t is the fluorescence having osmotic pressure π_t . The y intercept (f_b) is the background fluorescence, which indicates the proportion of intracellular calcein insensitive to external osmolarity. Figure 1 shows the changes in relative cell volume resulting from a 50% hypertonic challenge and the subsequent restoration of isotonic conditions following the abovementioned correction procedure.

DATA ANALYSIS AND STATISTICS

The raw data were corrected for fluorescence drift independent of cell volume changes (Hamann, 2002). Plots are V_t/V_0 , as a function of time, where V_t is the cell volume at time t ; V_0 is the initial cell

Fig. 2. Hypertonicity-induced RVI. (A) Relative cell volume was first determined in isotonic solution (300 mOsm) before changing to hypertonic solution: 375 (□), 450 (●), and 525 (Δ) mOsm at 37°C. (B) Temperature dependence of RVI in response to 50% hypertonic challenge at 24 (□), 32 (*), and 37°C (▲). (C) Linear fit curve of the relationship between relative cell volume of HCE cells and the bathing solution osmolarity ranging from 375 to 575 mOsm at 37°C. Data points are representative of six independent experiments ($N = 6$). Error bars indicate the standard error of the mean (SEM). Error bars are not shown when smaller than the symbols.

volume. The percentage (%) of RVI and RVD recovery was calculated as $(V_{\max} - V_f)/(V_{\max} - V_0) \times 100$; where V_{\max} is maximum volume change during the challenge and V_f is final volume.

Data were statistically analyzed with ORIGIN™ 6.1 software. Statistical significance was determined using Student's two-tailed t -test to determine significance ($P < 0.05$). Data were plotted as mean value \pm the standard error of the mean (SEM).

Results

HYPERTONICITY-INDUCED RVI

Figure 2A shows RVI behavior induced by step increases in bathing solution osmolarity at 37°C. Initially, relative cell volumes decreased by 15 ± 2 , 32 ± 3 , and $52 \pm 2\%$ during exposure to 375, 450, and 525 mOsm, respectively, followed by an RVI during such challenges. The initial shrinkage occurred relatively rapidly with a time constant (τ_{cO}) of 3 ± 0.5 min compared to the subsequent RVI to restore isotonic volume ($\tau_{cRVI} = 19 \pm 2.5$ min). Due to the significant difference between τ_{cO} and τ_{cRVI} from Fig. 2A, we used the minimal observed cell volume for validation of “fluorescence-volume” calibration. Figure 2C shows the dependence of minimal observed cell volume on the applied anisosmotic challenge.

We also found that RVI response is temperature-dependent. Lowering the temperature from 37 to 32°C delayed the RVI. Further temperature reduction to 24°C, reduced RVI by $59 \pm 4\%$ ($P < 0.001$) (Fig. 2B).

HYPOTONICITY-INDUCED RVD

The time-dependent increases in relative cell volume and RVD responses as a function of dilution of the bathing solution are shown in Fig. 3. The initial osmotic swelling required less than 30 s. The maximum cell volume increases were 14 ± 3 , 21 ± 3 , 37 ± 4 , and $53 \pm 7\%$ following dilution to 264, 225, 150, and 75 mOsm, respectively. Subsequently, RVDs restored initial volumes with a time constant of 2.5 ± 0.5 min. Within 10 min after the beginning of the osmotic shift, shrinkage reached levels that were below the initial isotonic volumes, and after another 25 min,

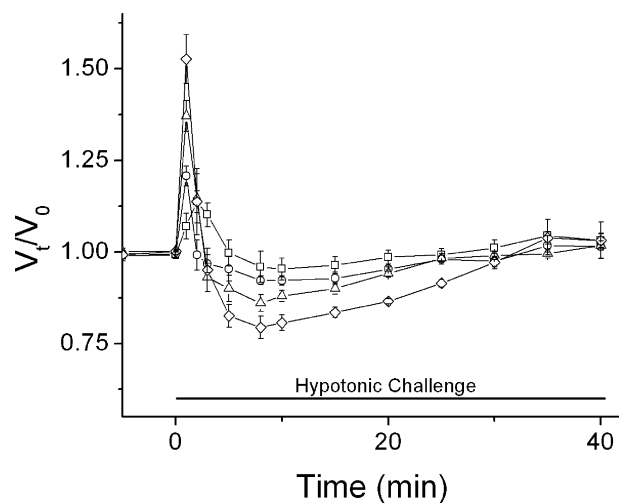
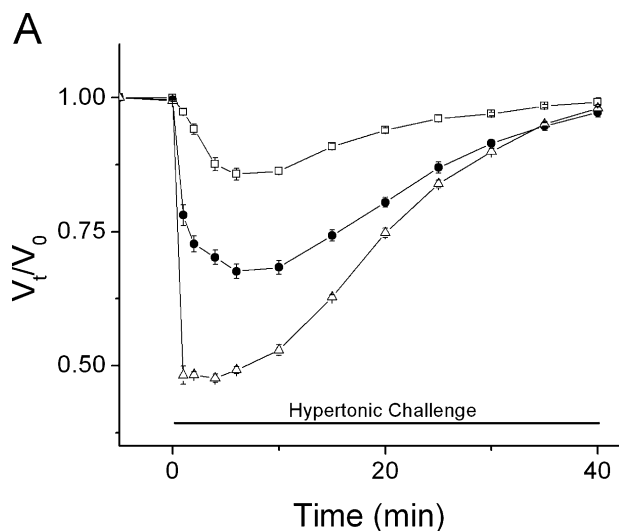
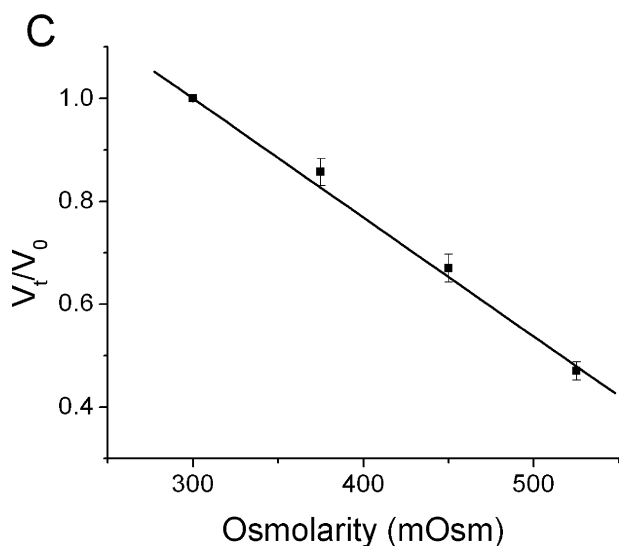
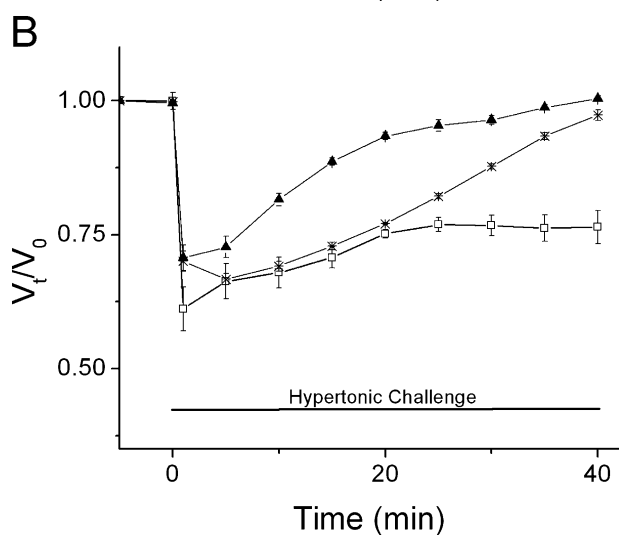


Fig. 3. Hypotonicity-induced RVD. After initial exposure to isotonic solution (300 mOsm), HCE cells were exposed to 264 (\square), 225 (\circ), 150 (Δ), or 75 (\diamond) mOsm hypotonic solution at 37°C. Data are presented as the mean \pm SEM ($N = 6$).



this overcompensation was followed by complete recoveries to their isotonic values. The observable maximal swelling, which is composed of osmotic response and the RVD response after 30 s, is almost

identical to the calculated values based on the decreases in solution osmolarity, which can be taken as an indication that RVD onset is somewhat delayed. A decrease in solution temperature to 24°C did not affect the time course of the RVD response (*data not shown*).

ISOTONIC VOLUME REGULATION

We found that using the selective NKCC inhibitor bumetanide (50 μM), has no significant effect on the isotonic steady-state cell volume (Fig. 4A and B). Similarly, we found that the selective $\text{Na}^+\text{-K}^+$ pump inhibitor, ouabain (1 mM), has a limited effect on isotonic cell volume in our setting. It produced an initial relative cell volume increase of $9 \pm 1\%$ ($P < 0.05$), which vanished within 20 min.

On the other hand, inhibition of K^+ conductance with 1 mM 4-AP (4-amino pyridine) induced an initial $20 \pm 3\%$ cell volume increase, which stabilized at 8% after 25 min. In the case of the Cl^- channel inhibition with DIDS (1 mM), it induced a maximum cell swelling of $26 \pm 2\%$ with subsequent relaxation to 9% after 25 min. A noteworthy finding is that inhibition by DIOA (100 μM) caused the relative isotonic volume to increase by $31 \pm 2\%$, which stabilized at 20% above baseline level after another 15 min. The role of KCC activity in the maintenance of this function is further indicated by the effect of the KCC activator NEM (1 mM). This activator induced a $52 \pm 4\%$ transient cell volume shrinkage.

INHIBITION OF REGULATORY VOLUME INCREASE

The effects of several inhibitors on RVI were evaluated under a 50% hypertonic challenge (450

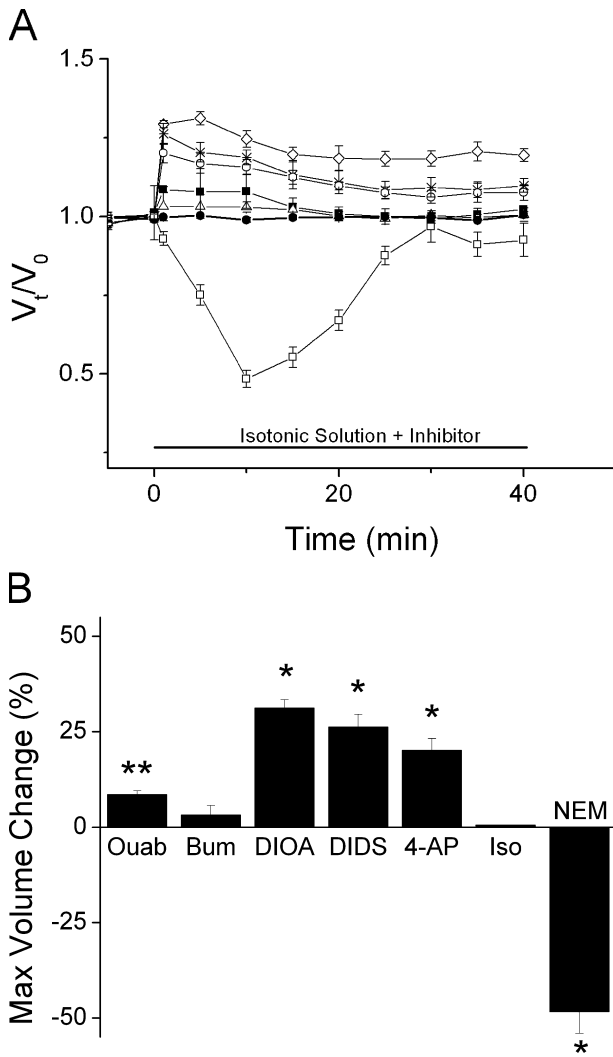
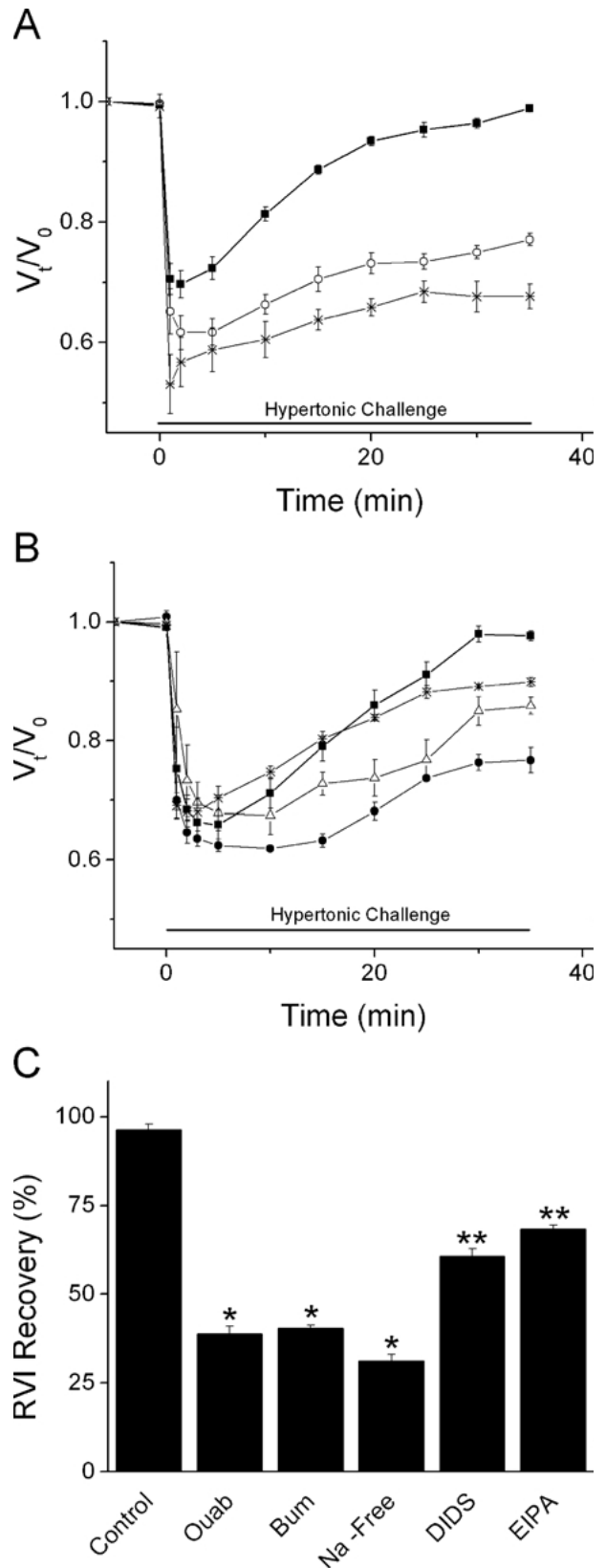


Fig. 4. Isotonic volume regulation. (A) After initial exposure to isotonic conditions, the following reagents were added in isotonic solution: 50 μM bumetanide (Δ), 1 mM ouabain (\blacksquare), 100 μM DIOA (\diamond), 1 mM DIDS (*), 1 mM 4-AP (\circ), and 1 mM NEM (\square) at 37°C. Untreated cells (\bullet) in isotonic solution are shown for comparison. Data are presented as the mean \pm SEM ($N = 6$). Error bars are not shown when smaller than the symbols. (B) Summary of maximum volume changes of the isotonic volume created by above reagents. * $P < 0.001$; ** $P < 0.05$ versus isotonic control.

mOsm) in HCE cells. As previously mentioned, untreated cells showed complete regulation (100% RVI). As shown in Fig. 5A, bumetanide (50 μM) suppressed the extent of RVI by $60 \pm 1\%$ ($P < 0.001$). In the absence of Na^+ , the extent of RVI was reduced by $69 \pm 2\%$ ($P < 0.001$). Figure 5B shows that ouabain (1 mM) inhibited the RVI response to a 450 mOsm challenge by $61 \pm 2\%$ ($P < 0.001$). With the inhibitors of $\text{Cl}^-/\text{HCO}_3^-$ (1 mM DIDS) and Na^+/H^+ (100 μM EIPA) exchangers, the relative cell volume recovery in response to a hypertonic challenge was partially inhibited by



$39 \pm 2\%$ ($P < 0.05$) and $32 \pm 1\%$ ($P < 0.05$), respectively (Fig. 5B and C).

Fig. 5. Regulatory volume increase inhibition at 37°C. (A) After initial exposure in isotonic solution, untreated HCE cells (■) and cells treated with the NKCC inhibitor 50 μM bumetanide (○) or bathing in Na⁺-free solution (*) were exposed to 50% hypertonic challenge. (B) Untreated HCE cells (■) and cells treated with the inhibitors 1 mM ouabain (●), 1 mM DIDS (Δ) and 100 μM EIPA (*) during a 50% hypertonic challenge. Data are presented as the mean ± SEM (*N* = 6). Error bars are not shown when smaller than the symbols. (C) Summary of relative RVI recovery (%) from data displayed in Fig. 5A and B. **P* < 0.001; ***P* < 0.05 versus control untreated cells during 50% hypertonic challenge.

INHIBITION OF REGULATORY VOLUME DECREASE

As shown in Fig. 6, untreated cells showed complete regulation (100% RVD). Initially, exposure to a 150 mOsm challenge induced swelling that reached a value $37 \pm 4\%$ above its relative isotonic volume. As increases in K⁺ efflux underlie RVD in numerous other cell types, we employed inhibitors of this pathway to assess its contribution to this response. The results shown in Fig. 6A and B indicate the inhibitory efficacy of 1 mM 4-AP, 100 μM glybenclamide, 10 mM TEA and 5 mM BaCl₂. The largest inhibitory effect ($42 \pm 3\%$; *P* < 0.001) was obtained with 4-AP, whereas BaCl₂ was the least effective ($27 \pm 4\%$; *P* < 0.05). A point worth noting is that in the presence of most K⁺ conductance inhibitors the initial swelling increased (range from 19 to 26%; *P* < 0.001) during a hypotonic challenge compared with untreated cells. With BaCl₂, the initial swelling was increased only by 6%. A more specific test for K⁺ efflux involvement in mediating RVD was to evaluate the initial increase in relative cell volume induced by a 150 mOsm challenge in a high-K⁺ (20 mM) solution. The initial cell volume increase in response to the hypotonic challenge was 26% higher than in untreated cells, which is similar to the increase observed in 4-AP-treated cells. This high-K⁺ hypotonic stress suppressed RVD by $52 \pm 3\%$.

The role of Cl⁻ in maintaining electroneutrality during K⁺ egress was evaluated by determining the effect of isosmolar substitution of bathing solution Cl⁻ with cyclamate. As indicated in Fig. 7A and B, such a change reduced the RVD response induced by a 50% hypotonic challenge to a value that is $58 \pm 3\%$ (*P* < 0.001) of the control value. Another approach to make this assessment entailed determining the inhibitory effects on RVD of described Cl⁻ channel blockers. RVD was partially inhibited by 1 mM DIDS and 100 μM niflumic acid by $47 \pm 2\%$ (*P* < 0.001) and $42 \pm 2\%$ (*P* < 0.001), respectively, suggesting that K⁺ loss is accompanied by Cl⁻ egress during RVD. Consistent with a role for Cl⁻ efflux, the initial swelling induced by this challenge was significantly higher in the presence of 1 mM DIDS ($48 \pm 6\%$) relative to untreated cells ($36 \pm 4\%$).

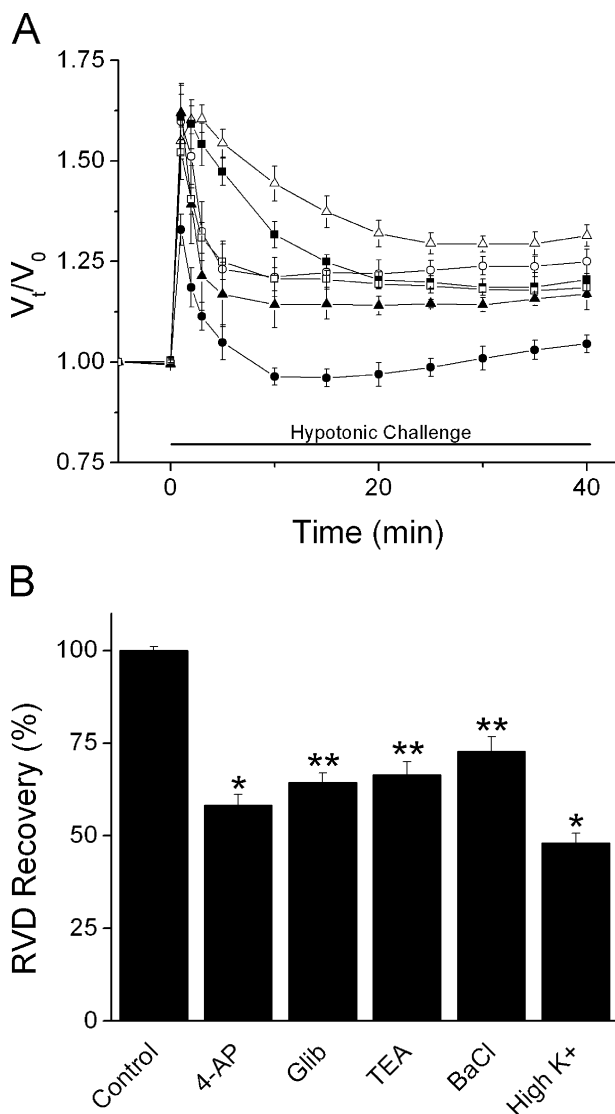


Fig. 6. Regulatory volume decrease inhibition by K⁺ channel blockers. (A) Hypotonic challenge (50%) to untreated cells (●), in the presence of high K⁺ (20 mM) 50% hypotonic solution (Δ) and after treatment with K⁺ channel inhibitors: 1 mM 4-AP (○), 10 mM TEA (■), 100 μM glybenclamide (□), and 5 mM BaCl₂ (▲). Data are presented as the mean ± SEM (*N* = 6). Error bars are not shown when smaller than the symbols. (B) Summary of relative declines in RVD recovery (%) caused by K⁺ conductance blockers. **P* < 0.001; ***P* < 0.05 versus control untreated cells during hypotonic challenge.

We determined that KCC activity contributes to RVD in HCE cells. DIOA is a non-diuretic agent with the capacity to block KCC transport without inhibiting NKCC activity when used below 200 μM (Diecke & Beyer-Mears, 1997; Culliford et al., 2003; Shen et al., 2003, 2004). The results in Fig. 8A indicate that DIOA (100 μM) blocked the RVD by $34 \pm 2\%$ (*P* < 0.001). During a 150 mOsm hypotonic challenge, DIOA induced an initial swelling response ($66 \pm 5\%$; *P* < 0.001) that was 33% greater than that induced by the challenge alone. DIOA

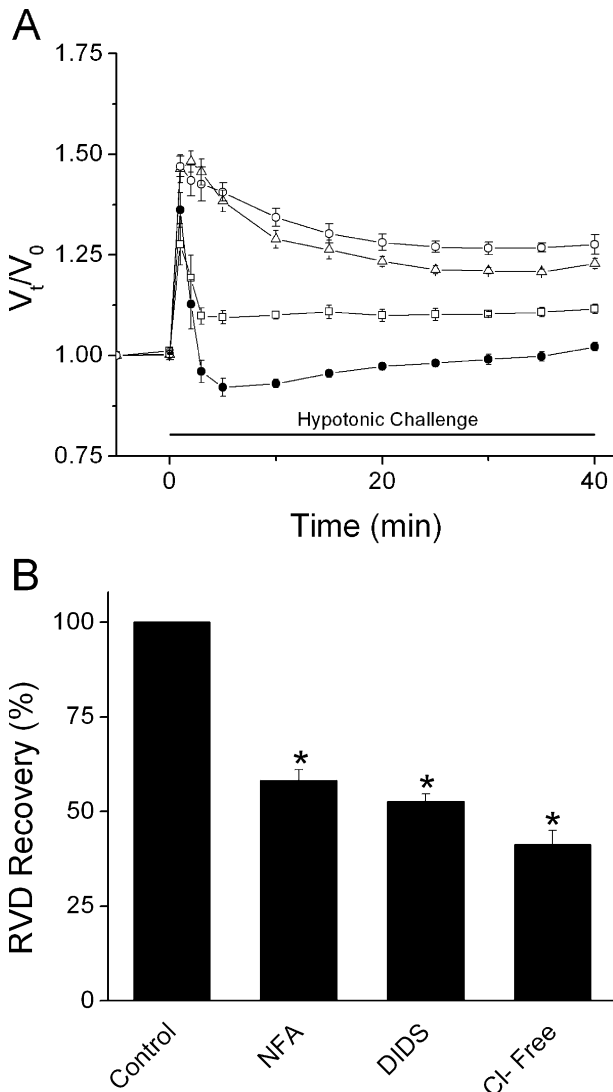


Fig. 7. Regulatory volume decrease inhibition by Cl^- channel blockers. (A) Hypotonic challenge (50%) to untreated cells (\bullet), and cells treated with Cl^- channel blockers: 1 mM DIDS (Δ), 100 μM niflumic acid (\square), or Cl^- -free solution (\circ). Data are presented as the mean \pm SEM ($N = 6$). Error bars are not shown when smaller than the symbols. (B) Summary of relative declines in RVD recovery (%) caused by Cl^- conductance blockers. * $P < 0.001$ versus control untreated cells during hypotonic challenge.

produced inhibition of RVD comparable to the average decline induced by the K^+ (42%) and Cl^- (47%) channel blockers (Fig. 8B). This similarity suggests the parallel participation of KCC in the RVD process. Furthermore, the KCC activator NEM (1 mM) induced $52 \pm 4\%$ ($P < 0.001$) cell volume shrinkage when added under isotonic condition, suggesting KCC expression in these cells. The initial cell shrinkage caused by a transient increase in KCl extrusion through KCC activity was followed by the recovery of the relative cell volume to near baseline levels after 34 min (Fig. 4A).

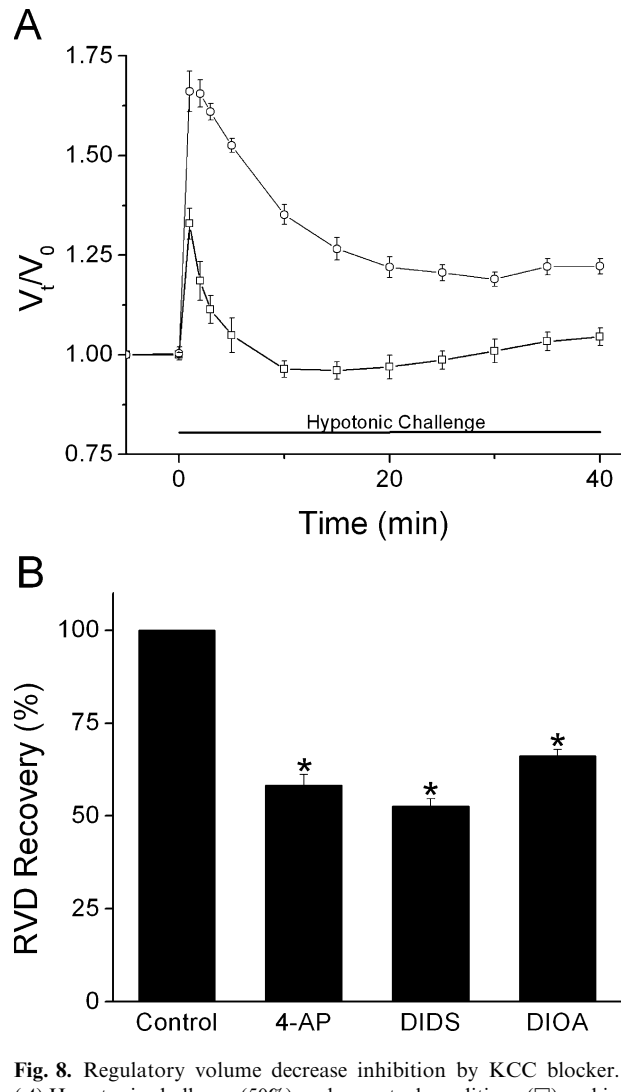


Fig. 8. Regulatory volume decrease inhibition by KCC blocker. (A) Hypotonic challenge (50%) under control conditions (\square) and in the presence of 100 μM DIOA (\circ). Data are presented as the mean \pm SEM ($N = 6$). (B) Summary of relative declines in RVD recovery (%) in the presence of the most effective K^+ and Cl^- conductance blockers, and a KCC inhibitor. * $P < 0.001$ versus control untreated cells during hypotonic challenge.

REGULATORY VOLUME BEHAVIOR CHARACTERIZATION BY FLUORESCENCE MICROSCOPY

The volume transients induced by anisotonic challenges were also characterized using fluorescence microscopy. Figure 9 shows the response to consecutive 150 mOsm and 450 mOsm challenges at 37°C . This hypotonic challenge initially induced $41 \pm 4\%$ cell swelling and triggered a complete RVD response to baseline isotonic volume ($\tau_c = 2.5 \pm 0.5$ min). On the other hand, during this hypertonic challenge there was an initial $27 \pm 1\%$ cell shrinkage followed by a slower volume recovery towards the pre-challenge isotonic condition ($\tau_c = 13 \pm 1.5$ min). After 20 min, the recovery was not yet complete. At this time, cell volume had reached 90% of the isotonic relative

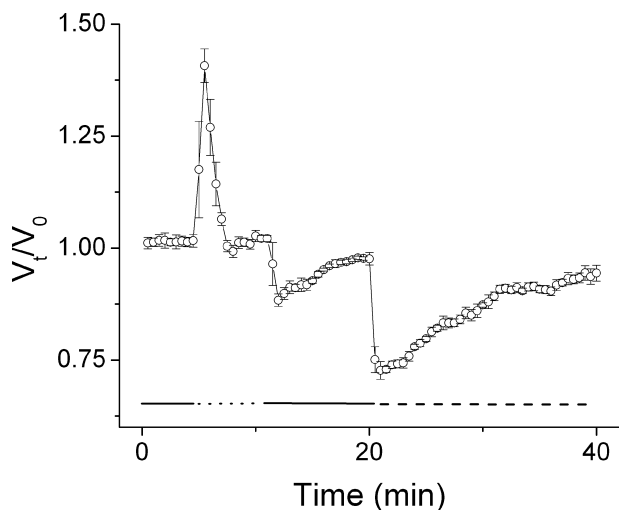


Fig. 9. Regulatory volume behavior characterization by fluorescence microscopy. Representative curve of relative cell volume vs. time of nine calcein-loaded cells from the same preparation attached to a coverslip at 37°C. Initially, cells were continually superfused with isotonic solution (*first solid line*) and subsequently exposed to hypotonic (150 mOsm) solution (*dotted line*). After hypotonically-adapted cells recovered to their original isotonic volume, cells were re-exposed to isotonic solution (*second solid line*). Subsequently, cells were exposed to a hypertonic (450 mOsm) challenge (*dashed line*). Data are presented as the mean \pm SEM.

volume, which is similar to the RVI time constant observed with the microplate analyzer.

Discussion

The ion transport mechanisms underlying regulatory volume behavior have been extensively characterized in a number of different cell types using single-cell fluorescence microscopy in combination with calcein quenching to monitor relative cell volume changes. Although, there are divided opinions as to how calcein quenching occurs, namely, either one due to a change in cell volume (self-quenching, Hamann, 2002, vs. intracellular protein quenching, Solenov et al., 2004), all agree that calcein is an excellent fluorophore to measure cell volume. Fluorescence microscopy has limitations because data acquisition is laborious, inefficient and the results are open to possible misinterpretation due to confounding errors, such as dye bleaching because of high light intensity excitation, inability to perform paired experiments, and low throughput capability. In this study, we were able to effectively overcome these drawbacks with the use of a fluorescence microplate analyzer, while obtaining similar regulatory volume responses under a specific condition.

In addition, the relative volume changes and regulatory volume behavior time course observed with this new approach are qualitatively similar to

those previously obtained with light scattering (Wu et al., 1997; Bildin et al., 2000, 2003; Al-Nakkash et al., 2004). However, there are substantial differences in the kinetics and extent of volume regulation between these two methods. For example, light scattering detected a faster initial volume regulation that was not evident in our study with calcein fluorescence quenching (Wu et al., 1997; Bildin et al., 2000, 2003; Al-Nakkash et al., 2004). The subsequent slower responses detected by light scattering could reflect the fact that they include changes in other non-volume related parameters (i.e., surface topology, cell junction) that contaminate cell volume measurements. The characterization of regulatory volume behavior with a fluorescence microplate analyzer also has the advantage of solely monitoring relative volume behavior rather than other confounding factors.

In the case of a hypertonic challenge, the time delay for the onset of RVI was longer than that for RVD response to hypotonic challenge. The latter response was almost immediate, making it difficult to distinguish an osmometric change from the RVD responses. Regardless of the technique used to characterize regulatory volume behavior, an assessment of the kinetic parameters of this response necessitates resolving the osmometric change in volume from the regulatory volume response. Such separation is needed to obtain a meaningful calibration of the relationship between changes in fluorescence and relative cell volume. We chose for this resolving process to analyze the time-dependent changes in relative cell volume induced by hypertonicity (Fig. 2C).

The difference between these time constants shown for RVD (~ 2.5 min) and RVI (~ 19 min) in Figs. 2A and 3 suggests that the cells are less poised to rapidly respond to a hypertonic than a hypotonic challenge. Another indication in support of this view is that hypotonically-induced swollen cells were initially able to regulate their volumes within 5 min and then overshoot their baseline levels followed by a slow return to their original isotonic volumes. Another possible reason for the slower RVI response is that the full complement of ion transporters mediating this response is not resident in the plasma membrane at the time of challenge. On the contrary, rapid RVD responses suggest that the ion transport mechanisms (i.e., KCC and separate K^+ and Cl^- channels) are already resident in the plasma membrane or located proximally in the cytoplasm. Alternatively, we expect that the RVD mechanism, which seems to be mostly dependent on ion channel opening, can quickly induce this response since channels have a larger ionic throughput than coupled NKCC, $Na^+ - K^+$ pump, and the Cl^- / HCO_3^- and Na^+ / H^+ exchangers' activities. Furthermore, we found that RVI is temperature-dependent (Fig. 2B). The RVI response was significantly attenuated when temperature was decreased from 37 to 24°C. Our finding of

temperature-dependent RVI is in agreement with prior studies in ciliary epithelial cells (Walker et al., 1999) and glioma cells (Mountian, Chou & Van Driessche, 1996). On the other hand, RVD is not temperature-dependent over this range (*data not shown*). In addition, such dependence is consistent with the notion that inwardly directed osmolyte uptake is maintained by metabolic support, whereas RVD occurs more rapidly, since intracellular K^+ and Cl^- levels are above electrochemical equilibrium and poised for release prior to a hypotonic challenge.

NKCC, Na^+-K^+ pump, and Cl^-/HCO_3^- and Na^+/H^+ exchangers contribute to RVI (Fig. 10). This identification is based on agreement between the effects of isosmolar single ionic substitutions and pharmacological modulators (Figs. 5–8). Similar to the results obtained with light scattering technique in RCE cells (Bildin et al., 1998, 2003), our results indicate that hypertonically-induced RVI is dependent on NKCC and Na^+-K^+ pump activities, since this response was blunted by nearly 60% in the presence of their respective inhibitors. Furthermore, there is a lesser degree of involvement of Cl^-/HCO_3^- and Na^+/H^+ exchangers in the RVI process.

On the other hand, our results indicate that K^+ and Cl^- efflux pathways are important mediators of RVD behavior induced by a hypotonic challenge in HCE cells (Figs. 6 and 7). This also suggests that Cl^- efflux is an essential anion accompanying K^+ efflux. The larger inhibitory effect exerted by high K^+ solution than by any K^+ efflux inhibitor on RVD further suggests the involvement of an additional mechanism for K^+ extrusion during acute hypotonic stress. We have two lines of functional evidence demonstrating that KCC plays an important role in the RVD response. First, the RVD response can be partially inhibited by DIOA (Fig. 8A). Second, the KCC activator NEM significantly activated KCC under isotonic conditions (Fig. 4A). Taken together, these results suggest that two different mechanisms are operative in HCE cells during hypotonically-induced RVD; parallel K^+ and Cl^- channels and KCC. This dual mechanism for RVD has been observed in several other cell types, including human retinal pigmented epithelial cells (Thornhill & Laris, 1984; Hoffmann & Simonsen, 1989; Kennedy, 1994).

Chloride and potassium channels, and the K^+-Cl^- cotransporter contribute to maintaining cell volume under isotonic conditions, since the inhibitors DIDS, 4-AP and DIOA significantly affected steady-state cell volume (Fig. 4A). On the other hand, the inhibition of the Na^+-K^+ pump and NKCC did not result in a significant isotonic volume alteration, which suggests that at least NKCC is not involved in maintaining the isotonic cell volume or its functions can be compensated for by another mechanism of volume regulation (Fig. 4A). We have incorporated our results with those previously described in corneal

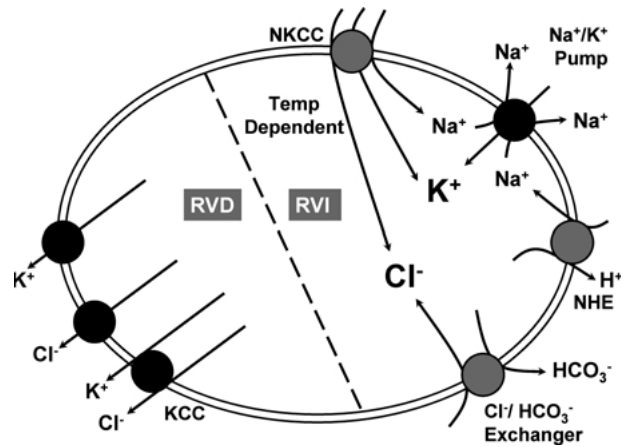


Fig. 10. Tentative model of ion transport mechanisms underlying RVI and RVD in corneal epithelial cells. The arrows indicate the net fluxes of ions for the specific pathway. The ion transport systems involved in RVI and RVD were separated for clarity. The black-filled circles indicate the ion transport mechanisms responsible for maintaining isotonic volume.

epithelial cells (Reinach et al., 1994; Diecke & Beyer-Mears, 1997; Wu et al., 1997; Takahira et al., 2001; Bildin et al., 2003; Lu et al., 2003; Al-Nakkash et al., 2004; Levin & Verkman, 2005) to provide a working model of the ionic mechanisms underlying regulatory volume behavior responsible for maintaining steady-state volume in corneal epithelial cells (Fig. 10).

In summary, HCE cells have the capacity to regulate their volume after acute anisotonic perturbation by activating in concert ion transport mechanisms and channels. RVI is temperature-dependent and is achieved mainly by the activation of the NKCC and the Na^+-K^+ pump, whereas there is also some involvement of Cl^-/HCO_3^- and Na^+/H^+ exchangers in this process. In contrast, K^+ and Cl^- channels are the dominant pathways mediating RVD along with the KCC activation. Our use of a fluorescence microplate analyzer to monitor time-dependent relative cell volume changes in calcein-loaded cells is a convenient and reliable technique.

This work was supported by National Institute of Health (NIH) grant EY04795

References

- Al-Nakkash, L., Iserovich, P., Coca-Prados, M., Yang, H., Reinach, P.S. 2004. Functional and molecular characterization of a volume-activated chloride channel in rabbit corneal epithelial cells. *J. Membrane Biol.* **201**:41–49
- Alvarez-Leefmans, F.J. 1995. Use of ion-selective microelectrodes and fluorescent probes to measure cell volume. *Meth. Neurosci.* **27**:361–391
- Araki-Sasaki, K., Ohashi, Y., Sasabe, T., Hayashi, K., Watanabe, H., Tano, Y., Handa, H. 1995. An SV40-immortalized human corneal epithelial cell line and its characterization. *Invest. Ophthalmol. Vis. Sci.* **36**:614–621

- Bildin, V.N., Wang, Z., Iserovich, P., Reinach, P.S. 2003. Hypertonicity-induced p38MAPK activation elicits recovery of corneal epithelial cell volume and layer integrity. *J. Membrane Biol.* **193**:1–13
- Bildin, V.N., Yang, H., Crook, R.B., Fischbarg, J., Reinach, P.S. 2000. Adaptation by corneal epithelial cells to chronic hypertonic stress depends on upregulation of Na:K:2Cl cotransporter gene and protein expression and ion transport activity. *J. Membrane Biol.* **177**:41–50
- Bildin, V.N., Yang, H., Fischbarg, J., Reinach, P.S. 1998. Effects of chronic hypertonic stress on regulatory volume increase and Na-K-2Cl cotransporter expression in cultured corneal epithelial cells. *Adv. Exp. Med. Biol.* **438**:637–642
- Bonanno, J.A. 1991. K(+)-H+ exchange, a fundamental cell acidifier in corneal epithelium. *Am. J. Physiol.* **260**:C618–C625
- Bonanno, J.A., Klyce, S.D., Cragoe, E.J. Jr 1989. Mechanism of chloride uptake in rabbit corneal epithelium. *Am. J. Physiol.* **257**:C290–C296
- Candia, O.A. 2004. Electrolyte and fluid transport across corneal, conjunctival and lens epithelia. *Exp. Eye Res.* **78**:527–535
- Culliford, S., Ellory, C., Lang, H.J., Englert, H., Staines, H., Wilkins, R. 2003. Specificity of classical and putative Cl(–) transport inhibitors on membrane transport pathways in human erythrocytes. *Cell Physiol. Biochem.* **13**:181–188
- Di Fulvio, M., Lauf, P.K., Shah, S., Adragna, N.C. 2003. NONOates regulate KCl cotransporter-1 and -3 mRNA expression in vascular smooth muscle cells. *Am. J. Physiol.* **284**:H1686–H692
- Di Fulvio, M., Lincoln, T.M., Lauf, P.K., Adragna, N.C. 2001. Protein kinase G regulates potassium chloride cotransporter-3 expression in primary cultures of rat vascular smooth muscle cells. *J. Biol. Chem.* **276**:21046–21052
- Diecke, F.P., Beyer-Mears, A. 1997. A mechanism for regulatory volume decrease in cultured lens epithelial cells. *Curr. Eye Res.* **16**:279–288
- Echevarria, M., Kuang, K., Iserovich, P., Li, J., Preston, G.M., Agre, P., Fischbarg, J. 1993. Cultured bovine corneal endothelial cells express CHIP28 water channels. *Am. J. Physiol.* **265**:C1349–C1355
- Farris, R.L. 1994. Tear osmolarity—a new gold standard? *Adv. Exp. Med. Biol.* **350**:495–503
- Fischbarg, J., Maurice, D.M. 2004. An update on corneal hydration control. *Exp Eye Res.* **78**:537–541
- Geck, P., Pietrzyk, C., Burckhardt, B.C., Pfeiffer, B., Heinz, E. 1980. Electrically silent cotransport on Na+, K+ and Cl– in Ehrlich cells. *Biochim. Biophys. Acta* **600**:432–447
- Grinstein, S., Dupre, A., Rothstein, A. 1982. Volume regulation by human lymphocytes. Role of calcium. *J. Gen. Physiol.* **79**:849–868
- Hamann, S., Kiilgaard, J.F., Litman, T., Alvarez-Leefmans, F., Wintr, B.R., Zeuthen, T. 2002. Measurement of cell volume changes by fluorescence self-quenching. *J. Fluoresc.* **12**:139–145
- Hoffmann, E.K., Simonsen, L.O. 1989. Membrane mechanisms in volume and pH regulation in vertebrate cells. *Physiol. Rev.* **69**:315–382
- Huhtala, A., Mannerstrom, M., Alajuuma, P., Nurmi, S., Toimela, T., Tahti, H., Salminen, L., Uusitalo, H. 2002. Comparison of an immortalized human corneal epithelial cell line and rabbit corneal epithelial cell culture in cytotoxicity testing. *J. Ocul. Pharmacol. Ther.* **18**:163–175
- Itoh, R., Kawamoto, S., Miyamoto, Y., Kinoshita, S., Okubo, K. 2000. Isolation and characterization of a Ca(2+)-activated chloride channel from human corneal epithelium. *Curr. Eye Res.* **21**:918–925
- Joiner, C.H., Rettig, R.K., Jiang, M., Franco, R.S. 2004. KCl cotransport mediates abnormal sulfhydryl-dependent volume regulation in sickle reticulocytes. *Blood* **104**:2954–2960
- Kennedy, B.G. 1994. Volume regulation in cultured cells derived from human retinal pigment epithelium. *Am. J. Physiol.* **266**:C676–C683
- Kregenow, F.M. 1971. The response of duck erythrocytes to hypertonic media. Further evidence for a volume-controlling mechanism. *J. Gen. Physiol.* **58**:396–412
- Lauf, P.K., Zhang, J., Delpire, E., Fyffe, R.E., Mount, D.B., Adragna, N.C. 2001. K-Cl co-transport: immunocytochemical and functional evidence for more than one KCC isoform in high K and low K sheep erythrocytes. *Comp. Biochem. Physiol. A Mol. Integr. Physiol.* **130**:499–509
- Levin, M.H., Verkman, A.S. 2005. CFTR-regulated chloride transport at the ocular surface in living mice measured by potential differences. *Invest. Ophthalmol. Vis. Sci.* **46**:1428–1434
- Linderholm, H. 1954. On the behavior of the sodium pump in from skin at various concentrations of Na ions in the solution on the epithelial side. *Acta Physiol. Scand.* **31**:36–61
- Lu, L., Wang, L., Shell, B. 2003. UV-induced signaling pathways associated with corneal epithelial cell apoptosis. *Invest Ophthalmol. Vis. Sci.* **44**:5102–5109
- Lytle, C., McManus, T. 2002. Coordinate modulation of Na-K-2Cl cotransport and K-Cl cotransport by cell volume and chloride. *Am. J. Physiol.* **283**:C1422–C1431
- McManus, M., Fischbarg, J., Sun, A., Hebert, S., Strange, K. 1993. Laser light-scattering system for studying cell volume regulation and membrane transport processes. *Am. J. Physiol.* **265**:C562–C570
- Mountian, I., Chou, K.Y., Van Driessche, W. 1996. Electrolyte transport mechanisms involved in regulatory volume increase in C6 glioma cells. *Am. J. Physiol.* **271**:C1041–C1048
- Pardo, L.A. 2004. Voltage-gated potassium channels in cell proliferation. *Physiology (Bethesda)* **19**:285–292
- Rae, J.L., Dewey, J., Rae, J.S. 1992. The large-conductance potassium ion channel of rabbit corneal epithelium is blocked by quinidine. *Invest. Ophthalmol. Vis. Sci.* **33**:286–290
- Reinach, P., Ganapathy, V., Torres-Zamorano, V. 1994. A Na:H exchanger subtype mediates volume regulation in bovine corneal epithelial cells. *Adv. Exp. Med. Biol.* **350**:105–110
- Roderick, C., Reinach, P.S., Wang, L., Lu, L. 2003. Modulation of rabbit corneal epithelial cell proliferation by growth factor-regulated K+ channel activity. *J. Membr. Biol.* **196**:41–50
- Russell, J.M. 2000. Sodium-potassium-chloride cotransport. *Physiol. Rev.* **80**:211–276
- Shen, M.R., Chou, C.Y., Hsu, K.F., Hsu, Y.M., Chiu, W.T., Tang, M.J., Alper, S.L., Ellory, J.C. 2003. KCl cotransport is an important modulator of human cervical cancer growth and invasion. *J. Biol. Chem.* **278**:39941–39950
- Shen, M.R., Chou, C.Y., Hsu, K.F., Liu, H.S., Dunham, P.B., Holtzman, E.J., Ellory, J.C. 2001. The KCl cotransporter isoform KCC3 can play an important role in cell growth regulation. *Proc. Natl. Acad. Sci. USA* **98**:14714–14719
- Shen, M.R., Droogmans, G., Eggermont, J., Voets, T., Ellory, J.C., Nilius, B. 2000. Differential expression of volume-regulated anion channels during cell cycle progression of human cervical cancer cells. *J. Physiol.* **529**:385–394
- Shen, M.R., Lin, A.C., Hsu, Y.M., Chang, T.J., Tang, M.J., Alper, S.L., Ellory, J.C., Chou, C.Y. 2004. Insulin-like growth factor 1 stimulates KCl cotransport, which is necessary for invasion and proliferation of cervical cancer and ovarian cancer cells. *J. Biol. Chem.* **279**:40017–40025
- Solenov, E., Watanabe, H., Manley, G.T., Verkman, A.S. 2004. Sevenfold-reduced osmotic water permeability in primary

- astrocyte cultures from AQP-4-deficient mice, measured by a fluorescence quenching method. *Am. J. Physiol.* **286**:C426–C432
- Strange, K. 2004. Cellular volume homeostasis. *Adv. Physiol. Educ.* **28**:155–159
- Takahira, M., Sakurada, N., Segawa, Y., Shirao, Y. 2001. Two types of K^+ currents modulated by arachidonic acid in bovine corneal epithelial cells. *Invest. Ophthalmol. Vis. Sci.* **42**:1847–1854
- Taouil, K., Hannaert, P. 1999. Evidence for the involvement of K^+ channels and K^+ - Cl^- cotransport in the regulatory volume decrease of newborn rat cardiomyocytes. *Pfluegers Arch.* **439**:56–66
- Thornhill, W.B., Laris, P.C. 1984. KCl loss and cell shrinkage in the Ehrlich ascites tumor cell induced by hypotonic media, 2-deoxyglucose and propranolol. *Biochim. Biophys. Acta* **773**:207–218
- Torres-Zamorano, V., Ganapathy, V., Reinach, P. 1993. Characterization and subtype identification of the Na^+ - H^+ exchanger in bovine corneal epithelium. *Curr. Eye Res.* **12**:69–76
- Verkman, A.S. 2000. Water permeability measurement in living cells and complex tissues. *J. Membrane Biol.* **173**:73–87
- Walker, V.E., Stelling, J.W., Miley, H.E., Jacob, T.J. 1999. Effect of coupling on volume-regulatory response of ciliary epithelial cells suggests mechanism for secretion. *Am. J. Physiol.* **276**:C1432–C1438
- Wang, L., Chen, L., Jacob, T.J. 2000. The role of ClC-3 in volume-activated chloride currents and volume regulation in bovine epithelial cells demonstrated by antisense inhibition. *J. Physiol.* **524**:63–75
- Wang, L., Chen, L., Zhu, L., Rawle, M., Nie, S., Zhang, J., Ping, Z., Kangrong, C., Jacob, T.J. 2002. Regulatory volume decrease is actively modulated during the cell cycle. *J. Cell Physiol.* **193**:110–119
- Wang, L., Fyffe, R.E., Lu, L. 2004. Identification of a $Kv3.4$ channel in corneal epithelial cells. *Invest. Ophthalmol. Vis. Sci.* **45**:1796–1803
- Wang, L., Li, T., Lu, L. 2003. UV-induced corneal epithelial cell death by activation of potassium channels. *Invest. Ophthalmol. Vis. Sci.* **44**:5095–5101
- Williams, K.K., Watsky, M.A. 2004. Bicarbonate promotes dye coupling in the epithelium and endothelium of the rabbit cornea. *Curr. Eye Res.* **28**:109–120
- Wu, X., Yang, H., Iserovich, P., Fischbarg, J., Reinach, P.S. 1997. Regulatory volume decrease by SV40-transformed rabbit corneal epithelial cells requires ryanodine-sensitive Ca^{2+} -induced Ca^{2+} release. *J. Membrane Biol.* **158**:127–136